

Quasi-static and dynamic tensile behaviors in electron beam welded Ti-6Al-4V alloy

ZHANG Jing¹, TAN Cheng-wen^{1,2}, REN Yu¹, WANG Fu-chi¹, CAI Hong-nian¹

1. School of Materials Science and Engineering, Beijing Institute of Technology, Beijing 100081, China;

2. Laboratory of Advanced Materials Behavior Characteristics,

Beijing Institute of Technology and Institute of Space Medico-Engineering, Beijing 100081, China

Received 11 December 2009; accepted 23 March 2010

Abstract: The quasi-static and dynamic tensile behaviors in electron beam welded (EBW) Ti-6Al-4V alloy were investigated at strain rates of 10^{-3} and 10^3 s^{-1} , respectively, by materials test system (MTS) and reconstructive Hopkinson bars apparatus. The microstructures of the base metal (BM) and the welded metal (WM) were observed with optical microscope. The fracture characteristics of the BM and WM were characterized with scanning electronic microscope. In Ti-6Al-4V alloy joint, the flow stress of WM is higher than that of BM, while the fracture strain of WM is less than that of BM at strain rates of 10^3 and 10^{-3} s^{-1} , respectively. The fracture strain of WM has apparent improvement when the strain rate rises from 10^{-3} to 10^3 s^{-1} , while the fracture strain of BM almost has no change. At the same time, the fracture mode of WM alters from brittle to ductile fracture, which causes improvement of the fracture strain of WM.

Key words: Ti-6Al-4V alloy; electron beam welding; quasi-static tensile behavior; dynamic behavior; fracture mode

1 Introduction

Titanium and its alloys are widely used in aeronautical industry, marine industry and petrochemical industry, etc[1–3], due to their intrinsic properties such as super high specific strength, good oxidation resistance, excellent corrosion resistance and good fatigue properties. Ti-6Al-4V alloy which is a α - β titanium alloy is one of the most popularly utilized titanium alloys[4–7]. In practice, applications frequently require the welding of various components to reduce the cost and difficulty of the machining process. However, rapid heating and cooling and filler material fusion into the weld metal (WM) often lead to inhomogeneous metallurgical and mechanical conditions in the welded joints, even if the filler metal is the same as the base metal (BM) [8]. The thermal effects associated with the welding process usually cause the failure of a structure at its welded joints [9]. Consequently, the welding characteristics of Ti-6Al-4V alloy play a very important role in the material selection for a specific application where welding is needed.

Furthermore, in automotive, aerospace, energy and

defense applications, the structures with weldment are often subjected to dynamic loading in service, such as explosion and impact of foreign objects. Hence, the understanding of dynamic characteristics on the behavior of the welded joints is also very important for the design of structures. In previous studies, there were reports available on mechanical properties (impact toughness, quasi-tensile properties and fatigue life, etc), fracture characterization of titanium alloys and their welds. MA et al[10] reported the microstructures, impact toughness and fracture characteristics of linear friction welded Ti-6Al-4V alloy joint. KISHORE et al[11] studied the room temperature hardness, quasi-static tensile properties and fatigue life of the Ti-6Al-4V weldment in the as-welded and post-weld heat treatment at two different temperatures. However, in these previous researches, most mechanical properties of the welded joints were tested under quasi-static loading conditions; little work concerned the dynamic mechanical behaviors, especially the dynamic tensile behavior of welded Ti-6Al-4V alloy.

In this study, material test system (MTS) and a reconstructive split Hopkinson tensile bars apparatus were used to evaluate and compare the mechanical

properties of the BM and WM of Ti-6Al-4V welded joints under quasi-static and dynamic loading conditions. The characterization of fracture surface was also considered.

2 Experimental

The material used in this experiment is conventional Ti-6Al-4V alloy sheet with nominal chemical composition Ti-6.09Al-4.02V-0.011C-0.14Fe-0.008N-0.14O-0.002 3H (mass fraction, %). Coupons with size of 65 mm×48 mm×5 mm cut from the sheet were mechanically wire brushed, acid pickled in an HF solution and subsequently cleaned with acetone prior to welding. Autogenously full penetration bead-on-plate electron beam weldments were made on coupons by electron beam welding (EBW), which would provide high quality weld joint because of high vacuum environment. The welding test was performed with midsize electron beam welding machine (MEDARD43 type produced by TECHMETA Company), and the parameters are listed in Table 1.

Table 1 Welding parameters for electron beam welding of Ti-6Al-4V alloy

Beam voltage/ kV	Beam current/ mA	Heat input/ (J·mm ⁻¹)	Speed/ (mm·min ⁻¹)	Vacuum/ 10 ⁻² Pa	Work distance/ mm
50	20	50	1200	9.33	250

The BM and WM specimens of Ti-6Al-4V joint were prepared by mounting, grinding and polishing, etched in a solution of 88%H₂O+2%HF+10%HNO₃ (volume fraction) and the microstructures were characterized with optical microscope.

The quasi-static tensile test and dynamic tensile test are carried out with MTS and reconstructive Hopkinson tensile bar apparatus at strain rates of 10³ and 10⁻³ s⁻¹, respectively. The reconstructive split Hopkinson tensile bar apparatus mainly comprises an incident bar and a transmitted bar made of *d* 14 mm maraging steel, and a block made of duralumin. The specimen is put between the incident bar and the transmitted bar stuck with gluewater before being loaded by a tensile loading pulse generated by the drop hammer impacting the block. A full description of the apparatus and more experimental theories can be found in Refs.[12–13].

In order to examine the effect of the microstructure on tensile properties, the size of tensile test sample was designed to make the testing region of tensile test samples only contain the same microstructure. The size of the testing region is 4 mm×5 mm×1.2 mm. The specimen shape can be found in Ref.[13].

After quasi-static and dynamic tensile tests, the specimens were recovered and the fracture characteristics of the specimens were investigated with scanning electron microscope. The fracture characteristics of the BM and WM under different strain rates were compared.

3 Results

3.1 Microstructures

Fig.1(a) shows the optical micrograph of the BM, which is typical bimodal microstructure and consists of equiaxed primary α grains and α/β lamellar within prior β grains. The white and dark regions represent α and β phases in the optical micrograph. Fig.1(b) shows the optical micrograph of the WM which exhibits clearly acicular needle microstructure and is greatly different from the bimodal microstructure of the BM. High heat input in EBW technique increases the temperature upwards the melting point of the Ti-6Al-4V alloy and subsequently diffusional transformation is substituted by martensite transformation at high cooling rates in the vacuum environment after EBW process. The similar observations were obtained by SARESH[14].

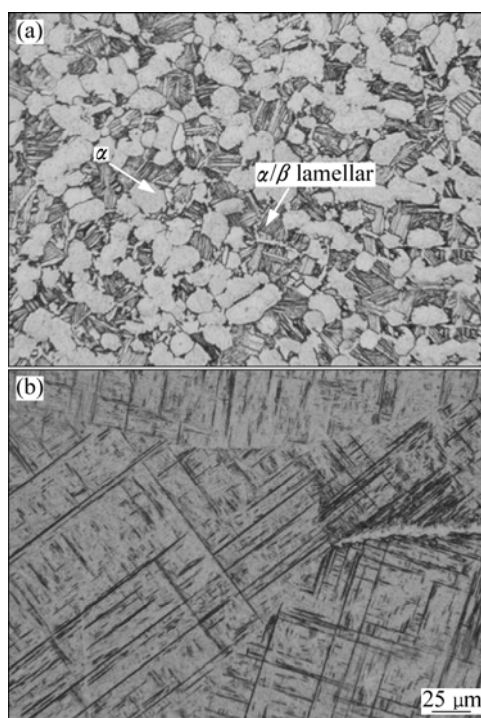


Fig.1 Optical micrographs of BM (a) and WM (b)

3.2 Quasi-static and dynamic tensile behaviors

The true stress—strain curves of the original BM and WM of the Ti-6Al-4V weld joint at strain rates of 10⁻³ and 10³ s⁻¹, respectively, are shown in Fig.2. Here, the elastic parts of all the stress—strain curves were expurgated to accurately compare the flow stress and

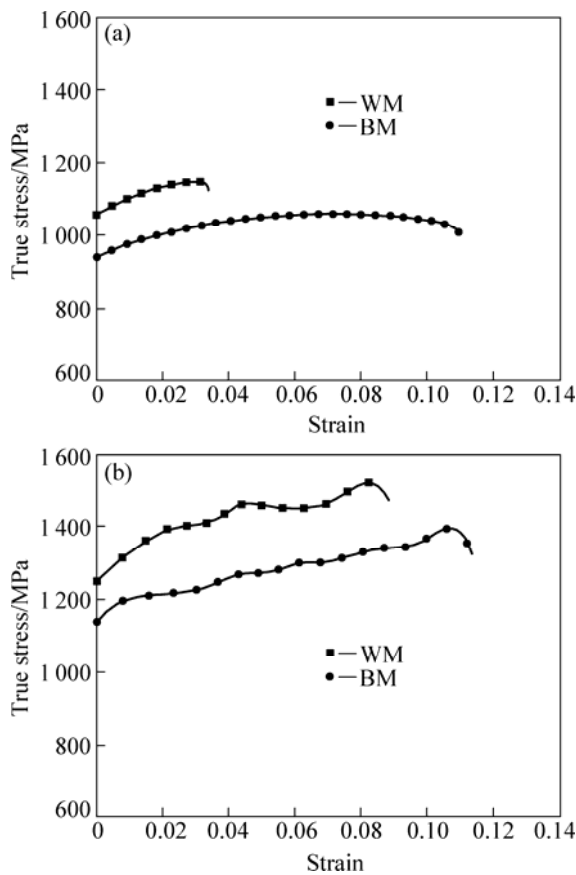


Fig.2 True stress—strain curves of WM and BM at strain rates of 10^{-3} (a) and 10^3 s^{-1} (b)

fracture strain between WM and BM at different strain rates.

Fig.2(a) shows the true stress—strain curves of BM and WM at the strain rate of 10^{-3} s^{-1} . It is found that the flow stress of WM is obviously higher (approximately average value of 120 MPa) than that of BM, while the fracture strain of WM is much lower (approximately 2.5%) than that of BM (approximately 11%). The dynamic tensile results at strain rate of 10^3 s^{-1} are shown in Fig.2(b). The flow stress of WM is still higher than that of BM (about 200 MPa), while the fracture strain of WM is lower than that of BM. As can be seen from Figs.2(a) and (b), the flow stress—strain behavior varies largely under the quasi-static and the dynamic conditions for both BM and WM. At a constant strain, the flow stress increases by about 200 MPa with an increase of strain rate. It is distinctly revealed that the WM is also strain rate dependent material as well as BM. It should be noted that the fracture strain of WM increases from approximately 2.5% to 8% when the strain rate increases from 10^{-3} to 10^3 s^{-1} , however, the fracture strain of the BM has almost no increase.

3.3 Fractographs

Fig.3 shows the fractographs of the tensile

specimens of BM and WM at strain rate of 10^{-3} s^{-1} . The SEM image of BM fracture surface exhibits a dimple-like and flocculent structure, indicating a typical ductile and transgranular fracture (Fig.3(a)). As known, titanium alloys contain essentially no inclusions, thus high strain concentration, which is expected to promote void coalescence type fracture, appears caused by microstructural features rather than inclusions. For the case of Ti-6Al-4V alloy, most of the BM ductile failures occurred during the process of void nucleation, growth and coalescence, and voids nucleation occurred mainly at the primary α/β interface[15]. Hence, the images reveal that the BM specimens ruptured with a ductile and transgranular fracture mode. By comparison, the SEM image of the WM fracture surface shows extensive faceting characterized by predominantly intergranular fractographic features at lower magnification (Fig.3(c)). Furthermore, at higher magnification, the SEM image of the WM fracture surface displays several cleavage planes and a small quantity of fine and shallow dimples (Fig.3(d)). The WM specimen shows typical brittle and intergranular fracture, although several dimples can be observed at higher magnification fractography.

Fig.4 shows the fractographies of the tensile specimens of BM and WM at a strain rate of 10^3 s^{-1} . In the case of BM specimen, the characterization of the fracture surface is similar to that of the specimen at a strain rate of 10^{-3} s^{-1} , as shown in Fig.4(a). Many fine dimples and tear ridges distributing over the fracture surface can be observed at higher magnification. In the case of WM specimen, the fractography at lower magnifications exhibits a brittle-like and relatively flat fracture surface. Here, analysis of titanium alloy fracture surfaces should be done cautiously, because at low magnifications, the relatively less ductile samples exhibit faceted appearance, indicating a cleavage type fracture. However, the fracture surface exhibits small and shallow dimples which are generally indicative of a ductile fracture because of the void coalescence observed at higher magnifications. In the present research, a large number of fine equiaxed dimples with diameter of 5–10 μm , appear obviously on the fracture surface at a strain rate of 10^3 s^{-1} , which implies a representative ductile fracture.

4 Discussion

In general, change of fracture modes is correlated with temperature and strain rate. Metals exhibit more brittle with decreasing temperature or increasing strain rate[16]. However, metals will show more ductile if the increasing strain rate exceeds a certain high value.

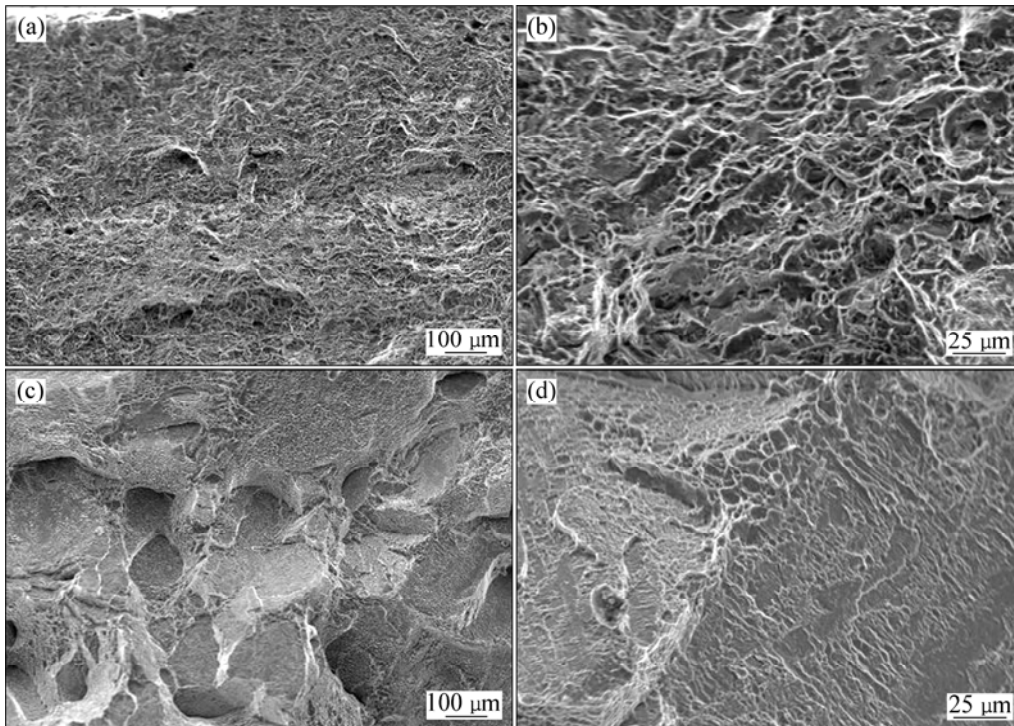


Fig.3 Fractographs of BM (a, b) and WM (c, d) at strain rate of 10^{-3} s^{-1}

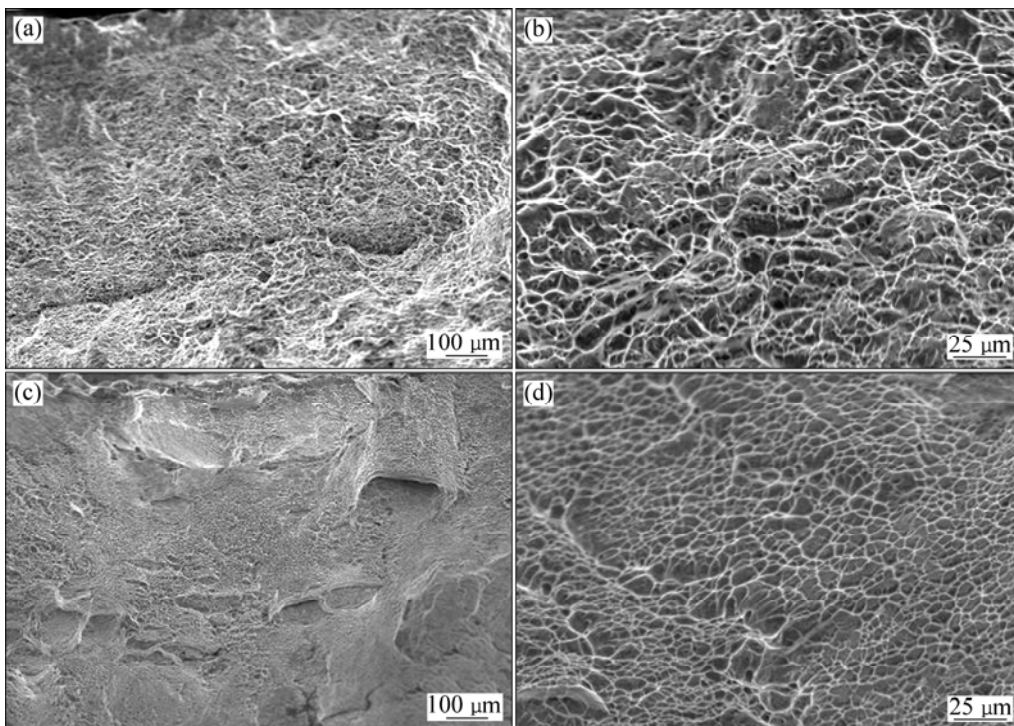


Fig.4 Fractographs of BM (a, b) and WM (c, d) at strain rate of 10^3 s^{-1}

Possible explanations for this phenomenon are: 1) Heat is generated in the material during plastic deformation and more deformation generates more heat; 2) At higher strain rate, the heat generated in the material has less time to dissipate to the surroundings. Therefore,

temperature is generally the main factor which affects the change of fracture modes during plastic deformation. It is widely known that under dynamic loading conditions, the adiabatic temperature rise during plastic deformation is also considered, which can be calculated

from

$$\Delta t = \frac{\eta}{\rho c_V} \int \sigma d\varepsilon \quad (1)$$

where ρ is the mass density (4.4g/cm^3); c_V is the heat capacity ($611\text{ J/(kg}\cdot\text{°C)}$); η is the fraction of plastic work converted into heat (η is 0.9). According to experimental data, the temperature rise in specimens of WM and BM at strain rate of 10^3 s^{-1} is calculated to be 50 and 58 °C, respectively. It is found that the temperature rise in BM is slightly higher than that in the WM. Observed from Figs.1(a) and (b), Fig.3(b) and Fig.4(b), the fracture strain of BM is almost not altered, which shows that the adiabatic temperature rise scarcely affects the fracture strain of BM at a strain rate of 10^3 s^{-1} . In contrast, for WM, both the improvement of fracture strain and change of fracture mode are noted, as described in section 3. However, no noticeable thermal softening is exhibited in dynamic tensile curves as seen from Fig.2, which implies that the temperature rise of 50 °C barely affects the fracture strain of WM. Hence, the temperature rise is not a main factor which affects the increase of fracture strain and the alternation of fracture mode in the present dynamic tensile results of WM. It is supposed that strain rate is another main factor affects the fracture strain and the change of fracture modes in quasi-static and dynamic tensile tests.

Analysis of WM fractographs under quasi-static and dynamic tensile conditions indicate that the fracture strain of WM is closely correlated to the fracture modes. Under the quasi-static tensile condition, the main factor determines that the fracture mode of WM specimens is grain-boundary strength which is low stress strength of the microstructure; while under dynamic tensile condition, it is intracrystalline strength which is high stress strength. It is presumed that the strength of grain-boundaries is enhanced with the elevated strain rate, which induces that the strength of grain-boundaries is above or equal to the intragranular strength. Consequently, deformation is no longer localized at the grain boundary and the fracture takes place through ductile and transgranular mode. Owing to the difference of the fracture modes under different tensile conditions, the quasi-static mechanical properties of WM after EBW process should not be simply utilized to evaluate the dynamic mechanical properties.

5 Conclusions

1) In Ti-6Al-4V alloy joint, the flow strength of the WM is higher than that of the BM, while fracture strain of the WM is lower than that of the BM at both strain rates of 10^3 and 10^{-3} s^{-1} . The fracture strain of WM has

apparent improvement when the strain rate increases from 10^{-3} to 10^3 s^{-1} , while the fracture strain of the BM has almost no change.

2) The fracture mode of WM alters from brittle to ductile fracture with increasing strain rate from 10^{-3} to 10^3 s^{-1} , which causes improvement of fracture strain of WM from quasi-static and dynamic tensile condition. Hence, the quasi-static mechanical properties of WM after EBW process should not be simply utilized to evaluate the dynamic mechanical properties, owing to the change of the fracture modes when loading condition changes from quasi-static condition to dynamic condition.

References

- [1] BOYER R R. An overview on the use of titanium in the aerospace industry [J]. *Mater Sci Eng A*, 1996, 213(1/2): 103–114.
- [2] BAO He-sheng, WANG Li-li, LU Wei-xian. The high velocity deformation and adiabatic shearing of a titanium alloy at low temperature [J]. *Explosion and Shock Wave*, 1989, 2: 109–119. (in Chinese)
- [3] YANG Yang, ZHANG Xin-ming, LI Zheng-hua, LI Qing-yun. Adiabatic shearing phenomenon of bonding layer in explosive clad titanium/mild steel [J]. *The Chinese Journal of Nonferrous Metals*, 1995, 5(2): 93–97. (in Chinese)
- [4] REDDY N S, LEE Y H, PARK CH H, LEE CH S. Prediction of flow stress in Ti-6Al-4V alloy with an equiaxed $\alpha+\beta$ microstructure by artificial neural networks [J]. *Mater Sci Eng A*, 2008, 492(1–2): 276–282.
- [5] LEE D G, LEE S H, LEE Y T. Effect of precipitates on damping capacity and mechanical properties of Ti-6Al-4V alloy [J]. *Mater Sci Eng A*, 2008, 486(1–2): 19–26.
- [6] ZUO J H, WANG Z G, HAN E H. Effect of microstructure on ultra-high cycle fatigue behavior of Ti-6Al-4V [J]. *Mater Sci Eng A*, 2008, 473(1–2): 147–152.
- [7] LIU X Q, TAN C W, ZHANG J, HU Y G, MA H L, WANG F C, CAI H N. Influence of microstructure and strain rate on adiabatic shearing behavior in Ti-6Al-4V alloys [J]. *Mater Sci Eng A*, 2009, 501(1–2): 30–36.
- [8] TANG W, SHI Y W. Influence of strength matching and crack depth on fracture toughness of welded joints [J]. *Eng Fract Mech*, 1995, 51(4): 649–659.
- [9] LEE D G, JANG K C, KUK J M, KIM I S. Fatigue properties of inertia dissimilar friction-welded stainless steels [J]. *J Mater Process Tech*, 2004, 155–156: 1402–1407.
- [10] MA T J, LI W Y, YANG S Y. Impact toughness and fracture analysis of linear friction welded Ti-6Al-4V alloy joints [J]. *Materials and Design*, 2009, 30(6): 2128–2132.
- [11] KISHORE B N, GANESH S R S, SRINIVASA M C V, MADHUSUDHAN R G. Effect of beam oscillation on fatigue life of Ti-6Al-4V electron beam weldments [J]. *Mater Sci Eng A*, 2007, 471(1–2): 113–119.
- [12] SONG J Z, XIA Y M. 3-D dynamic elastic-plastic FEA for rotating disk indirect bar-bar tensile impact apparatus: Numerical analysis for the generation of mechanically-filtered incident stress pulse [J]. *International Journal of Impact Engineering*, 2006, 32(8): 1313–1338.

- [13] WANG C Y, XIA Y M. Validity of one-dimensional experimental principle for flat specimen in bar-bar tensile impact apparatus [J]. Solids and Structures, 2000, 37(24): 3305–3322.
- [14] SARESH N, GOPALAKRISHNA P M, MATHEW J. Investigation into the effects of electron beam welding on thick Ti-6Al-4V titanium alloy [J]. J Mater Process Technol, 2007, 192–193: 83–88.
- [15] PRASAD R K, ANGAMUTHU K, BALA S P. Fracture toughness of electron beam welded Ti6Al4V [J]. J Mater Process Technol, 2008, 199(1–3): 185–192.
- [16] XU Z, LI Y. Dynamic behaviors of 0Cr18Ni10Ti stainless steel welded joints at elevated temperatures and high strain rates [J]. Mechanics of Materials, 2009, 41(2): 121–130.

电子束焊接 Ti-6Al-4V 合金的准静态和动态拉伸行为

张 静¹, 谭成文^{1,2}, 任 宇¹, 王富耻¹, 才鸿年¹

1. 北京理工大学 材料学院, 北京 100081;
2. 北京航天医学工程研究所 先进材料行为特性实验室, 北京 100081

摘 要: 利用传统拉伸试验机和霍普金森(Hopkinson)拉杆实验装置研究电子束焊接的 Ti-6Al-4V 合金在应变率为 10^{-3} 和 10^3 s^{-1} 时的准静态和动态拉伸行为, 利用光学显微镜和扫描电子显微镜观察基体材料和焊缝材料的微观组织, 研究基体材料和焊接材料在拉伸实验后的断裂特征。结果表明: 在应变率分别为 10^{-3} 和 10^3 s^{-1} 的条件下, 焊缝材料的强度明显高于基体材料, 焊缝材料的伸长率低于基体材料。同时, 焊缝材料和基体材料均为应变率敏感材料; 当应变率从 10^{-3} 上升到 10^3 s^{-1} 时, 焊缝材料的伸长率明显提高, 而基体材料的伸长率基本没有变化; 焊缝材料的断裂模式由脆性断裂转向韧性断裂, 造成从准静态加载条件到动态加载条件下焊缝材料伸长率的提高。

关键词: Ti-6Al-4V 合金; 电子束焊接; 准静态拉伸行为; 动态行为; 断裂模式

(Edited by FANG Jing-hua)